

NSGA-II Algorithm-Based Wide Area Measurement (WAMS) Allocation With Considering Reliability

Guimin Xu^{1*} and Zhengxiang Yang²

¹School of Physics and Mechanical & Electrical Engineering, Hubei University of Education, Wuhan 430205, China

²School of intelligent manufacturing, Wuhan Technical College of Communications, Wuhan 430065, China)

*Corresponding author. E-mail: bingfeng71@126.com

Received: Jun. 08, 2023; Accepted: Oct. 26, 2023

Today's power systems for various reasons, including linearization of equations of state estimation and improved speed control and protection systems, use Wide Area Measurement (WAMS). Due to their high cost, it is essential to optimize the number and placement of this equipment. The costs associated with deploying a Synchro phasor have evolved throughout time. The cost of upgrading a substation, which is far more than the cost of a single device, has emerged as the major expense component. When determining where to put phasor measuring units (PMUs), it's important to consider not only how many will need to be built at each substation but also how many will need to undergo upgrades to accommodate them. In this paper, the multi-functional locating of phasor measurement units has been done with goals such as the cost of investment and risk in power systems (reliability) by indicating the observability. Then the location of the phasor units was solved in the form of an optimization problem, using multi-objective optimization algorithm NSGA-II. In the end, the performance of the proposed method is examined on the 9-bus system.

Keywords: Observability of Power Systems; Optimal PMU Allocation; Power System Reliability; Risk Cost; NSGA-II Algorithm

© The Author(s). This is an open-access article distributed under the terms of the [Creative Commons Attribution License \(CC BY 4.0\)](https://creativecommons.org/licenses/by/4.0/), which permits unrestricted use, distribution, and reproduction in any medium, provided the original author and source are cited.

[http://dx.doi.org/10.6180/jase.202502_28\(2\).0016](http://dx.doi.org/10.6180/jase.202502_28(2).0016)

1. Introduction

Over the last few years, due to the growing charge and lack of adequate systems of production and transmission of electric energy, as well as the emergence of the issue of restructuring in the electricity industry, the complexity and density of the system load increased, and this reduced the margin of stability in power systems. Under such circumstances, it is important to estimate their exact state and thus ensure their stable performance of the system. Now this is usually done by Supervisory Control and Data Acquisition (SCADA) systems. The state estimation in this system is based on measurements that are not simultaneous with low sampling rate, and the most importantly thing is that it is not able to measure voltage and current phasor. As a result, operators will not have access to a dynamic state of

the system to be able to maintain system performance in critical situations [1, 2].

Power grid incident investigations have highlighted the significance of situational awareness and critical information at control centers for effective management of power system operations. If system operators had a better grasp on the comparable status of stressed power systems, disruptions may have been avoided or their effects mitigated in many cases [1]. Synchro phasor measurement technology (SMT) was identified as a potentially useful strategy for bolstering situational awareness. An unprecedented depth of insight into the state of today's electrical grids is provided [3-5]. The phasor measurement unit (PMU) [5] is the primary SI unit for SMT. Currently, SMT (sometimes referred to as a wide-area measurement system) is in charge

of keeping tabs on and regulating both static and dynamic power grids (WAMS).

As a result of developments in communication technology, phasor measuring devices are currently among the most important tools for WAMPCC (Wide Area Monitoring, Protection, and Control) in power grids. This equipment employs modern signal processing techniques, including GPS, to address these difficulties. Due to the high cost of equipment installation and the absence of suitable communication infrastructure, and given the fact that the PMU installed in each bus is capable of measuring phasor voltage and current of all lines connected to that bus, locating the lowest number to maintain the observability of the power system is one of the main goals of the projects related to systems [6]. In addition to the observability and state estimation, the phasor units use data to find the location of a fault in transmission lines [7]. In addition to the observability and state estimation, the phasor units use data to find the location of a fault in transmission lines [8], , and also in large-scale protection, adaptive transient relay, thermal monitoring of transmission lines and voltage sustainability [9, 10].

Statistical evaluation of power system reliability has rarely focused on the significance of monitoring and control systems. Wang et al. [11], the authors find a probabilistic case study assessing the reliability of Ontario Hydro's control center infrastructure as a whole. While this article looked at control room equipment failures, it didn't look at how SCADA system failures affect power system performance. Ghazizadeh and Aghamohammadi [12], a model that included SCADA and the power system assessed the impact of SCADA failures on load reductions in the power system. The idea was fantastic, but the execution was vague. While this study did include controllability limitations, it did not account for observability gaps in its analysis of power systems.

In Zima et al. [13], the uses of WAMS were investigated by analyzing a few simple case studies. Probability of successful operations was calculated based on the availability of WAMS elements. The probabilistic analyses of the electricity grid, however, were extremely preliminary. Multiple reliability indices for a regional WAMS network were computed in Wang et al. [14]. Failures of PMUs and communication links were accounted for; however, failures of measuring transformers and transmission cables were not. By providing a quantitative hardware reliability evaluation approach for the WAMS communication network and the WAMS as a whole, the authors enhance their prior work [15].

In Aminifar et al. [16], the observability of power net-

works based on WAMS was subjected to a probabilistic analysis. An index of probabilistic observability was created for buses connected to a particular PMU deployment setup. The system index that can be used to gain insight into the network's overall observability was found by taking the average of the bus indices. Both 16, Aminifar et al. [17] were created with PMU installation in power systems in mind, the former with a more detailed model. They did not, however, analyze how WAMS failures affect power system performance.

Studies have focused on the location of phasor units by considering factors such as uncertainty in the lines and phasor measuring units [18–21] or multi-objective optimization of phasor placement [22], while in Chakrabarti and Kyriakides [21] the positioning of phasor units was done by considering the impact of formulated lanes exit. Abbasy and Ismail [18] has studied the effect of the withdrawal of one or more of phasor units. On the other hand, Aminifar et al. [19] and Rakpenthai et al. [20] investigated the effect of simultaneous exit of lines and phasor units.

The contributions of this work can be summarized as follows:

1. Addressing Observability Gap: The authors tackle the challenge of observability in power systems, particularly focusing on the issue of maintaining observability while minimizing the number of Phasor Measurement Units (PMUs) installed. This is critical for efficient and cost-effective monitoring of power grids.

2. Integration of Risk Cost: Unlike previous studies, the authors incorporate the concept of risk cost, directly linking it with the reliability of the power system. By considering the impact of disturbances and failures, the authors provide a more comprehensive understanding of the cost-effectiveness of PMU placement.

3. Application of NSGA-II Algorithm: The authors employ the NSGA-II algorithm, a well-established multi-objective optimization method, for the optimal placement of PMUs. This algorithm allows us to balance multiple objectives effectively, such as observability, cost reduction, and risk mitigation.

This article compares the connection between the risk cost (reliability of the system) and the cost of adding phasor measurement devices. In addition to the observability of the whole network and decrease in the cost of installation, the authors can decrease the risk cost due to disturbance, which is not included in previous articles. Furthermore, NSGA-II algorithm was used for optimal placement of phasor measurement units. In the section 2 of this paper, positioning of phasor units is defined and the concept of observability of power systems is described. section 3 elab-

orates on the proposed algorithm has been studied. In section 4, the results of simulation and analysis are discussed, and the conclusion is expressed in the section 5.

2. Concept of observability and PMU ALLOCATION

2.1. Observability of Power systems

The estimation of network variables to estimate system state is generally understood to be the definition of the power system observability. If the network state estimation is calculated and if the grid state estimation encounters a problem, the network will not be observable [23]. The network variables are usually considered as buses phasor voltage. The magnitude and phase angle of a bus's voltage can be determined via phasor devices mounted on that bus. Additionally, they are able to determine the current phasor of each branch connected to that bus. As a result, utilizing the fundamentals of KVL and KCL of power, the magnitude and phase angle of voltage of buses connected to buses equipped with phasor measurement devices can be computed. Therefore, buses in which phasor measurement units are installed have direct observability, and buses connected to buses with phasor measurement units have indirect observability. Buses that do not have relationship with buses with phasor measurement units are not observable (Fig. 1).

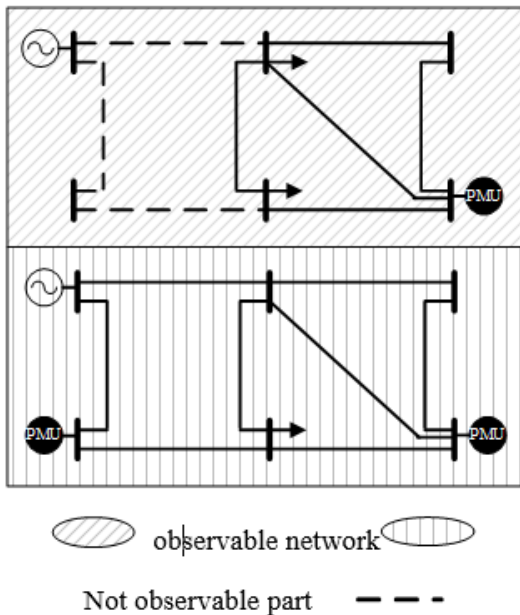


Fig. 1. Network observability using PMU

2.2. Formulation of PMU Allocation Problem

PMU installed in a bus can estimate the voltage phasor and current phasor of that bus as well as the voltage phasor of all branches connected to that bus. Thus, when PMU is installed at strategic points in the network, the information needed to observe the systems can be obtained. Estimating the network observability and reducing the number of PMU are the two main goals. In this paper, the location of phasor units is investigated so that in addition to the minimization of number of required units, the peripheral objectives including the largest number of observability and total observability of entire network can be fulfilled. The placement with respect to reliability should be in a way that if there is chance of disturbance, the observability of the network suffers from minimal disturbance.

For a system with n buses, the optimal location problem is expressed via the Eq. (1) [24]:

$$\begin{aligned} \min \sum_{i=1}^n w_i x_i & \quad (1) \\ \text{s.t } y = Ax \geq b & \end{aligned}$$

Where n is the number of buses in the system, w is the matrix of installed PMU costs or bus weight matrix that may change depending on the importance of each bus. It is often considered as the matrix n×n, and A and b are defined as follows:

$$A_{n \times n}(i, j) = \begin{cases} 1 & i = j \\ 1 & \text{if buses } i \text{ and } j \text{ are connected} \\ 0 & \text{otherwise} \end{cases} \quad (2)$$

$$x_{n \times 1}(i, j) = \begin{cases} 1 & \text{if PMU installed in bus } i \\ 0 & \text{other} \end{cases} \quad (3)$$

$$b = [1 \ 1 \ 1 \ 1 \ 1 \ \dots \ 1 \ 1]^T \quad (4)$$

The i^{th} row of matrix Ax in Eq. (1) represents the frequency of the observability of the i^{th} bus, which must be at least one, and is used for the full observability of the system.

3. Reliability of power systems

In traditional power system planning studies, the reliability of the network was a condition. This condition is assumed as certain and probabilistic in studies on composite system [25]. In certain cases, the reliability of power systems is calculated up to the maximum output of one or two elements. Due to few and easy application, this method is widely used in different studies. However, in renovated power systems, there are many uncertainties which cannot be considered by certain methods. Thus, today in many

articles and researches, probabilistic approach is used for reliability studies, which can model the uncertainty in the network [25]. In the probabilistic approach, indicating the reliability is expressed as follows:

$$EEENS_{TS,G} \leq EENS_R \tag{5}$$

$EEENS_{TS,G}$: Expected energy not supplied in bus due to exit transmission lines and generators.

$EENS_R$: The minimum desired level of Expected energy not supplied due to exit transmission lines and generators.

In studies on renovated environment, to attain optimal design not with minimum cost but with reasonable cost of load shedding, the standard reliability is used as an objective function [25]. In this paper, the risk cost (reliability) is as an objective, and decrease in the cost of installing PMU is another goal. Reliability is estimated by using Monte Carlo method.

3.1. Indexes of Reliability

A) Index load shedding or loss of load probability (LOLP) is expressed as Eq. (6):

$$LOLP = \sum_{C_i \neq 0} P_i \tag{6}$$

The P_i of certain load shedding is C_i .

B) The expected energy not supplied (EENS) is:

EENS: the lack of energy in a specific period of time.

The following equation estimates lack of energy in one year:

$$EENS = \sum_{C_i \neq 0} C_i \times P_i \times 8760 \tag{7}$$

In the above equation, C_i is the disconnected load, and P_i is the corresponding probability. This article uses EENS index, since it is a very important indicator to check the reliability.

3.2. Calculate Indexes Reliability Using Monte Carlo Methods

If the set S is a composite set of the states of the system components, $F(S)$ is the result of S mode test on the system. According to the probabilistic approach, for calculating indices of reliability, mathematical expectation of this index is calculated with respect to $F(S)$ in Eq. (8).

$$E(F) = \sum_{s \in X} F(s) \cdot P(s) \tag{8}$$

In this equation, overall states of the system calculated by Monte Carlo simulation is called X . For example, EENS index value is the numerical value of the mathematical expectation of the following two-valued function:

$$F(S) = \begin{cases} 1 & \text{if } x \text{ is a failed state} \\ 0 & \text{if } x \text{ is anormal state} \end{cases} \tag{9}$$

Mathematical expectation $E(F)$ for $F(s)$ is shown as follows:

$$\hat{E}(F) = \frac{1}{N} \sum_{i=1}^{NS} F(s_i) \tag{10}$$

The variance $E(F)$ is:

$$V(\hat{E}) = \frac{V(F)}{N} \tag{11}$$

And therefore, its estimated value is:

$$\hat{V}(F) = \frac{1}{N-1} \sum_{i=1}^N (F(s_i) - \hat{E}(F))^2 \tag{12}$$

The convergence of Monte Carlo method in each iteration is done by examining relationship in Eq. (13).

$$P \left(\lim_{N \rightarrow \infty} \left| \frac{1}{N} \sum_{i=1}^N F(s_i) - E(F) \right| = 0 \right) = 1 \tag{13}$$

$$P \left(\lim_{N \rightarrow \infty} \hat{E}(F) = E(F) \right) = 1 \tag{14}$$

In other words, the estimated value of $\hat{E}(F)$ of the reliability index with Monte Carlo method with probability 1 converges to $E(F)$ when $N \rightarrow \infty$.

3.3. DC Load Flow with Linear Programming

In this paper, minimizing the amount of disconnected load in each bus of the network is expressed in the form of Eq. (15).

$$\min \sum_{j=1}^{N_D} P_{Dj} \tag{15}$$

$$\text{s.t. } B\theta + P_L = P_G + P_D$$

$$\begin{aligned} \sum_{i=1}^{N_G} P_{Gi} + \sum_{i=1}^{N_D} P_{Di} &= \sum_{i=1}^{N_D} P_{Li} \\ \underline{P}_G &\leq P_G \leq \bar{P}_G \\ 0 &\leq P_D \leq P_L \\ |T| &\leq \bar{T} \end{aligned} \tag{16}$$

P_{Gi} power generate at bus i , P_{Di} Power demand at bus i , P_{Li} power loss at bus i .

4. Proposed algorithm of NSGA-II

The main features [26] of algorithm NSGA-II are:

- Use of a binary tournament selection operator.
- Definition of (Crowding Distance) as an alternative to techniques like fitness sharing.
- Storage and archiving of compromised solutions produced in the algorithm's earlier steps (elitism).

As shown in Fig. 2, and $F_1(X)$ and $F_2(X)$ are the space or values of our objective functions (the solutions to the problem). These solutions are ranked given that they are compromised. The priority is for first front optimal solutions, and if necessary, 2nd front will be used; and hence other solutions will be used in the same order.

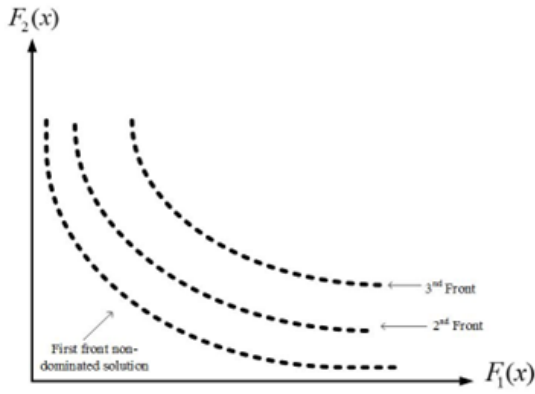


Fig. 2. Ranking of solutions based on the Pareto Front

Crowding Distance is more for less crowded areas and less in more crowded areas [26]. Crowding Distance is defined only between members of the front.

In Fig. 3, the answers are prioritized based on ratings. More crowding distance of the solutions means that they are better, and they will form our new population [26]. Since the size of our new population should be equal to the size of the initial population, some solutions will be rejected.

4.1. Final Fuzzy Decision

Fuzzy logic is a suitable method for determining the non-linear classification. Fig. 4 shows the membership function for a fuzzy variable [27]. μ is the importance of our objective functions. For example, when $\mu_{\text{investment cost}} = 0.6$, $\mu_{\text{Risk cost}} = 0.8$ it means that the minimization of the risk cost is more important than the minimization of the cost of phasor measurement units installation.

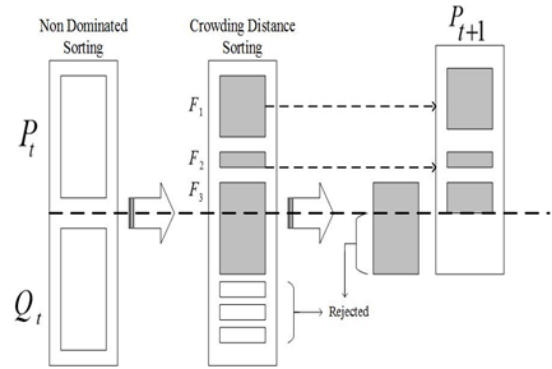


Fig. 3. Process that occurs in NSGA-II

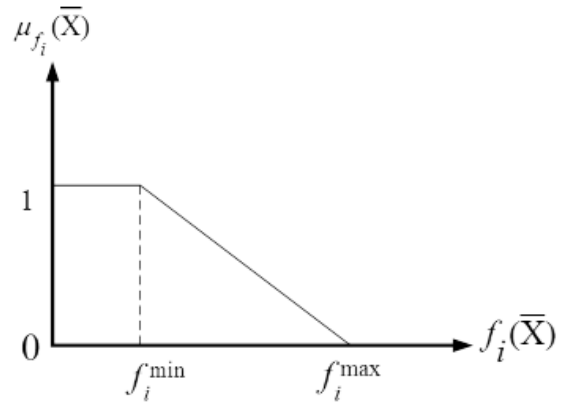


Fig. 4. Membership function for target functions

Because of the imprecise and uncertain decision over the receptors, the relevant objective function has a solution: $f_i(x)$ is expressed by the membership function: $\mu_i(x)$.

$$\mu_{f_i} = \begin{cases} 0 & f_i(X) > f_i^{\max} \\ \frac{f_i^{\max} - f_i(X)}{f_i^{\max} - f_i^{\min}} & f_i^{\min} \leq f_i(X) \leq f_i^{\max} \\ 1 & f_i(X) < f_i^{\min} \end{cases} \quad (17)$$

Where f_i^{\max} and f_i^{\min} are respectively the upper and lower limit of the i^{th} objective function. Therefore, the ultimate optimal solution is optimal with respect to the desired level (μ_{r_i}) can be achieved via the following optimization problem:

$$\min \sum_{X \in \Phi} |\mu_{r_i} - \mu_{f_i}|^p \quad P \in [1, \infty) \quad (18)$$

The flowchart of the proposed method (Fig. 5) is designed in a way that after the initial location (lowest number) is randomly selected condition, observability is investigated, and if the network is not observable, placement

will take place again. If the network is observable, the authors assume that disturbances (reliability) happen in the network (the authors are after states in which the network maintains its observability if in case of any disturbance). In this state, the authors check the observability and the best solutions will be saved until the desired reiteration is achieved.

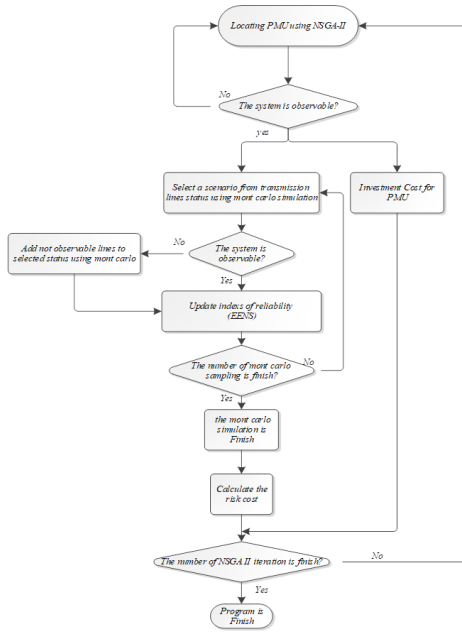


Fig. 5. Flowchart of proposed method

5. Results of simulation and analysis

The simulations in this paper were conducted using MATLAB on a computer with 16GB of RAM and an Intel Core i7 processor. The connections between the 9 buses in the system analyzed in this research are shown in Fig. 6. Tables 1 to 3 contain information for the 9-bus system. First, the PMUs are randomly placed in different buses via NSGA-II algorithm, and the objective function includes all costs of each PMU. The cost of PMUs is considered according to their channels [27]. Furthermore, the full observability of the system is calculated, and since the risk cost is important in investment, and the authors consider system reliability and start the simulation. Fig. 7 shows the distribution of solutions based on Pareto front.

Fig. 6 shows the three PMUs on buses 4, 6, and 8 that make up the WAMS network responsible for system monitoring/control. While buses 5, 7, and 9 offer redundant PMU measurements, these gadgets make the network entirely observable.

The information in Table 4 pertains to the reliability of

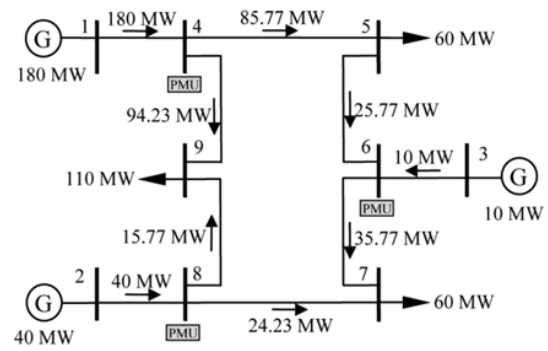


Fig. 6. Branches connection of 9-bus system and PMU Allocation

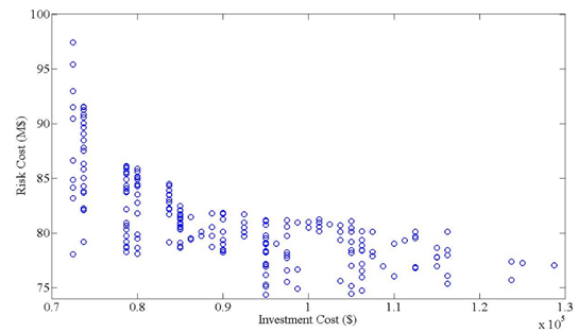


Fig. 7. Distribution of solutions based on Pareto front

Table 1. Information of Generators

	Generator location (Bus)		
	1	2	3
Accessibility	0.98	0.96	0.99
Min Output (MW)	0	0	0
Max Output (MW)	220	40	120
Base Output (MW)	180	40	10

Table 2. Information of Distributed Load

	Location (Bus)		
	9	7	5
Consumed Load (MW)	110	60	60
Percentage of Total %	47.82	26.09	26.09

WAMS devices. Phasor calculations involve observations in three phases [4]. For a PMU to calculate a current phasor, it requires a minimum of three functioning CTs, making their availability equal to 0.999584. This also applies to the required voltage phasor. The following situations are subject to research:

Table 3. Information of Transmission System

Branch		Power flow rate (Mw)	Accessibility	Reactance of line (pu)
From	To			
4	5	0.085	110	0.9952
4	9	0.140	160	0.9943
5	6	0.206	110	0.9905
1	4	0.170	250	0.9907
2	8	0.143	120	0.9965
3	6	0.189	140	0.9942
6	7	0.137	110	0.9976
7	8	0.241	55	0.9944
8	9	0.097	55	0.9954

Table 4. Reliability of WAMS Devices

Devices	Accessibility
Communication link	0.999
Current Transformer	0.999
PMU	0.995
Potential Transformer	0.998

Scenario 1, emergency power grid scenarios in which WAMS are available and trusted.

Scenario 2, The power grid and WAMS are subject to a small number of interdependent variables.

Scenario 3, both the electrical grid and WAMS fail.

5.1. Scenario 1

The effect of WAMS failures on power system reliability indices is measured under this scenario. In Table 5, the authors can see the load point and power system reliability indices. The highest load point index in this case belongs to bus 9. EDNS9’s index weight and PD9’s share of total system demand are only somewhat correlated (see Table 2). Furthermore, EDNS5 is much bigger than EDNS7, although PD5 is the same size as PD7. The load-shedding strategy in response to unforeseen events provides a plausible explanation for these findings.

Table 5. Scenario 1, Indexes of Reliability

	Location (Bus)			System
	9	7	5	
EDNS [MW]	1.699	0.178	0.386	2.263
Percentage of Total %	75.07	7.87	17.06	100

Scenario 2 Together, the power grid and WAMS are the focus of this scenario, which simulates their cooperative response to a variety of possible scenarios.

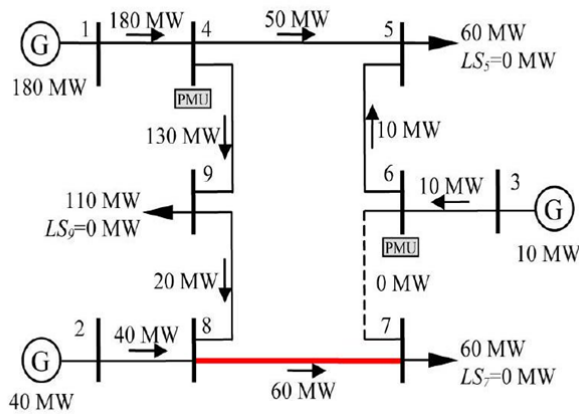
1) The protection and monitoring unit (PMU) at bus 4 and line 1-4 (or the generating unit at bus 1) is out of ser-

vice. This scenario simulates frequency instability and the potential for a power outage. In this scenario, the generation capacity of the system is 160 MW, and load shedding of at least 70 MW is required. Due to the malfunction of the WAMS, the system’s curtailable load at bus 7 is only 60 MW. As a result, the demand exceeds the generation and the system frequency decreases, causing a blackout. In reality, the automatic under-frequency shielding could limit the extensive effects of the disturbance. Include the protection model in the next version of the proposed reliability analyses.

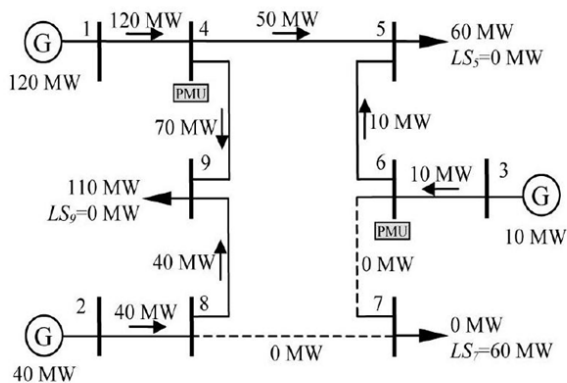
2) The PMUs for bus 6 and lines 1–4 are no longer in service. This scenario simulates the impact of WAMS availability on load shedding. This scenario is comparable to Contingency 1 from the standpoint of the power system. However, the failure of WAMS will have an impact on other components. In Condition 2, the load point on bus 9 and the transmission lines that connect to it are both controllable and observable. As a result, the 70MW loss in generation is offset by a fall in load at bus 9.

3) The PMU at bus stop 8 and lines 6-7 is offline. This situation simulates bus isolation and cascading failures. Bus lines 2-8, 7-8, and 8-9, as well as buses 2, 7, and 8 are not observable, according to the observability analysis. The power flow solution when lines 6-7 are down is shown in Fig. 8a. Bus 7 can only be supplied with the 60MW load through Line 7-8, which has a 55MW capacity. Line 7-8 is therefore overloaded even if it cannot be seen in the control room. As a result, lines 7-8 cause the safety system to trip. Bus 7 is isolated by the cascading event, which lowers the load. The 120MW drop in generating dispatch from unit 1 is necessary to accommodate the 60MW reduction in load. Following a cascading loss, the line flow is shown in Fig. 8b. Regardless of its unobservability in the control center, the cure for this contingency would be LS 7=5MW to relieve the line 7-8 overload, according to the conventional reliability evaluation.

4) Bus 2's generator and power management unit (PMU) are both offline. This backup plan simulates the situation in which the malfunctioning system is still operational. The system slack unit at bus 3 compensates for the generation loss caused by the breakdown of generating unit 2, and the new power flow solution does not exceed the transmission restrictions. Table 6 details the results of load shedding in Scenario 2.



(a) Outage before cascade



(b) Outage following a cascade

Fig. 8. Scenario 2, Condition 3: load flow after line 6-7 failure

Table 6. Load reductions of situations 1-4 in scenario 2

Buses	Load Shedding		
	9	7	5
Contingency 1	110	60	60
Contingency 2	70	0	0
Contingency 3	0	60	0
Contingency 4	0	0	0

5.2. Scenario 3

This scenario examines all potential outcomes, including the four states looked at in the preceding scenario, for the electricity system and the WAMS network. Table 7 displays the load points and system reliability indices. This scenario is comparable to Scenario 1, where it is assumed that the WAMS network is 100 percent reliable. Table 7, WAMS contingencies become worse. An extremely broad range, from 2.82% to 20.78%, characterizes the load point reliability index.

Table 7. Comparison between Scenarios 1 and 3's reliability indices

Buses	Load Shedding			System
	9	7	5	
Scenario 1	1.699	0.178	0.386	2.379
Scenario 3	1.747	0.215	0.417	2.12
% Difference	2.82	20.78	8.03	5.10

5.3. Effect of other parameters

This section explores two scenarios in which the unavailability of WAMS (see Table 4) is multiplied by a factor of 0.1 or 10 in Scenario 3. The first imitates a WAMS network that is incredibly reliable. Table 8 contrasts the outcomes of Scenario 3 with Scenario 8 findings. A less reliable WAMS could make the electricity system less dependable. According to Table 8, the OLS feasibility and its numerous solutions cause a significant variation in load point indices.

Deploying More PMUs: Increasing component availability may be too expensive or unattainable in general. It would be more pragmatic to incorporate redundant components [18]. To improve system observability in the event of a power system or WAMS failure, more PMUs can be connected to a WAMS system bus. In light of this, the authors recommend adding one more PMU to the nine-bus compact system. The additional PMU may be located on buses 1, 2, 3, 5, 7, or 9. There are so six distinct methods for installing four PMUs. The breakdown of the dependability index for the standard and novel placement strategies is presented in Table 9. Different PMU schemes offer varied degrees of enhancement.

The best approach is to add a PMU to bus 9, which is where the bulk load of the system is connected in Table 9. The second option is to add a PMU at bus 1 that is made up of the system's biggest generator. The next practical remedy is to put PMUs in buses 4, 4, 7, and 8. Due to bus 7's increased PMU, which lowers the possibility of isolation brought on by line overloads, it shows the most benefit in this approach.

Table 8. Indexes of reliability with a reliable WAMS

	Load Shedding			System
	5	7	9	
Scenario 3	0.317	0.205	1.647	2.279
Factor 0.1	0.289	0.171	1.607	2.177
% Difference	-5.71	-14.81	-2.18	-3.28
Factor 10	0.563	0.424	2.042	3.229
% Difference	57.99	141.7	21.61	38.93

Table 9. Indices of reliability for each of the four PMU placement strategies

PMU Placement	EDNS (MW)			System EDNS
	5	7	9	
4,6,8	0.317	0.205	1.647	2.279
1,4,6,8	0.302	0.179	1.628	2.229
2,4,6,8	0.304	0.211	1.631	2.236
4,6,7,8	0.308	0.212	1.624	2.234
4,6,8,9	0.289	0.163	1.611	2.183
3,4,6,8	0.320	0.207	1.642	2.279
4,5,6,8	0.308	0.213	1.625	2.236

Therefore, big units and/or loads on buses make them better candidates for PMU installation. However, the buses serving important or valuable loads are ideal for improving observability if the value of lost load (VOLL) or equivalently the interrupted energy assessment rate (IEAR) is taken into account in the power system reliability evaluation.

6. Conclusion

As the usage of measurement units in power systems increases, system monitoring should take advantage of this vital tool's exceptional reliability and inexpensive installation. This work has made possible the methodology for adding WAMS faults in power system reliability evaluation. Presumably, WAMS was responsible for the monitoring and/or control responsibilities. Using numerical research, the proposed method may model a scenario in which the WAMS network has problems and an event in power systems spreads as a result. Even though they may appear unlikely, such incidents could have a significant impact on load shedding and result in substantial changes to estimates of reliability. Typically, these incidents are not considered in standard evaluations of reliability. In this article, the effect of increased system reliability (reducing the risk cost) was examined. The authors also focused on the optimal placement of phasor measurement units when the cost of measurement unit installation is low. The simulation results showed that to increase the reliability, more measurement units are needed so that in Scenario of dis-

turbance, the observability is maintained. As mentioned earlier, the ideal situation is when the benefit from the difference of reducing the risk cost is more compared to the benefit from difference of the cost of installing measurement units.

References

- [1] A. P. S. Meliopoulos, G. J. Cokkinides, O. Wasynczuk, E. Coyle, M. Bell, C. Hoffmann, C. Nita-Rotaru, T. Downar, L. Tsoukalas, and R. Gao. "PMU data characterization and application to stability monitoring". In: IEEE, 2006, 8–pp.
- [2] S. Afzal, B. M. Ziapour, A. Shokri, H. Shakibi, and B. Sobhani, (2023) "Building energy consumption prediction using multilayer perceptron neural network-assisted models; comparison of different optimization algorithms" *Energy* **282**: 128446.
- [3] F. Aminifar, M. Fotuhi-Firuzabad, M. Shahidepour, and A. Khodaei, (2010) "Probabilistic multistage PMU placement in electric power systems" *IEEE Transactions on Power Delivery* **26**: 841–849.
- [4] M. Patel, S. Aivaliotis, and E. Ellen, (2010) "Real-time application of synchrophasors for improving reliability" *NERC report, Oct 1*: 4.
- [5] V. Terzija, G. Valverde, D. Cai, P. Regulski, V. Madani, J. Fitch, S. Skok, M. M. Begovic, and A. Phadke, (2010) "Wide-area monitoring, protection, and control of future electric power networks" *Proceedings of the IEEE* **99**: 80–93.
- [6] A. G. Phadke and J. S. Thorp. *Synchronized phasor measurements and their applications*. 1. Springer, 2008.
- [7] A. Khaleghi, M. O. Sadegh, and M. G. Ahsae, (2018) "Permanent Fault Location in Distribution System Using Phasor Measurement Units (PMU) in Phase Domain." *International Journal of Electrical Computer Engineering* (2088-8708) **8**:
- [8] C.-W. Liu and J. Thorp, (1995) "Application of synchronized phasor measurements to real-time transient stability prediction" *IEE Proceedings-Generation, Transmission and Distribution* **142**: 355–360.
- [9] T. T. Nguyen and V. L. Nguyen. "Application of wide-area network of phasor measurements for secondary voltage control in power systems with FACTS controllers". In: IEEE, 2005, 2927–2934.
- [10] A. G. Phadke, (1993) "Synchronized phasor measurements in power systems" *IEEE Computer Applications in power* **6**: 10–15.

- [11] L. Wang, P. P. Gelberger, and N. Ramani. "Reliability assessment of the operational functions of a power system control center". In: IET, 1991, 229–234.
- [12] M. S. Ghazizadeh and M. R. Aghamohammadi, (2023) "A Deep Learning-Based Attack Detection Mechanism against Potential Cascading Failure Induced by Load Redistribution Attacks" **IEEE Transactions on Smart Grid**:
- [13] M. Zima, M. Larsson, P. Korba, C. Rehtanz, and G. Andersson, (2005) "Design aspects for wide-area monitoring and control systems" **Proceedings of the IEEE** **93**: 980–996.
- [14] Y. Wang, W. Li, J. Lu, and H. Liu, (2009) "Evaluating multiple reliability indices of regional networks in wide area measurement system" **Electric Power Systems Research** **79**: 1353–1359.
- [15] Y. Wang, W. Li, and J. Lu, (2010) "Reliability analysis of wide-area measurement system" **IEEE Transactions on Power Delivery** **25**: 1483–1491.
- [16] F. Aminifar, M. Fotuhi-Firuzabad, M. Shahidehpour, and A. Khodaei, (2011) "Observability enhancement by optimal PMU placement considering random power system outages" **Energy Systems** **2**: 45–65.
- [17] F. Aminifar, M. Fotuhi-Firuzabad, M. Shahidehpour, and A. Khodaei, (2010) "Probabilistic multistage PMU placement in electric power systems" **IEEE Transactions on Power Delivery** **26**: 841–849.
- [18] N. H. Abbasy and H. M. Ismail, (2009) "A unified approach for the optimal PMU location for power system state estimation" **IEEE Transactions on power systems** **24**: 806–813.
- [19] F. Aminifar, A. Khodaei, M. Fotuhi-Firuzabad, and M. Shahidehpour, (2009) "Contingency-constrained PMU placement in power networks" **IEEE Transactions on Power Systems** **25**: 516–523.
- [20] C. Rakpenthai, S. Premrudeepreechacharn, S. Uatrongjit, and N. R. Watson, (2006) "An optimal PMU placement method against measurement loss and branch outage" **IEEE transactions on power delivery** **22**: 101–107.
- [21] S. Chakrabarti and E. Kyriakides, (2008) "Optimal placement of phasor measurement units for power system observability" **IEEE Transactions on power systems** **23**: 1433–1440.
- [22] K. Deb. *Multi-objective optimisation using evolutionary algorithms: an introduction*. Springer, 2011, 3–34.
- [23] J. B. A. London, S. A. R. Piereti, R. A. de Souza Benedito, and N. G. Bretas, (2009) "Redundancy and observability analysis of conventional and PMU measurements" **IEEE Transactions on Power Systems** **24**: 1629–1630.
- [24] F. Aminifar, C. Lucas, A. Khodaei, and M. Fotuhi-Firuzabad, (2009) "Optimal placement of phasor measurement units using immunity genetic algorithm" **IEEE Transactions on power delivery** **24**: 1014–1020.
- [25] F. Aminifar, M. Fotuhi-Firuzabad, and A. Safdarian, (2012) "Optimal PMU placement based on probabilistic cost/benefit analysis" **IEEE Transactions on Power Systems** **28**: 566–567.
- [26] D. Dua, S. Dambhare, R. K. Gajbhiye, and S. A. Soman, (2008) "Optimal multistage scheduling of PMU placement: An ILP approach" **IEEE Transactions on Power delivery** **23**: 1812–1820.
- [27] A. Khaleghi, M. O. Sadegh, M. Ghazizadeh-Ahsaei, and A. M. Rabori, (2018) "Transient fault area location and fault classification for distribution systems based on wavelet transform and adaptive neuro-fuzzy inference system (ANFIS)" **Advances in Electrical and Electronic Engineering** **16**: 155–166.